Non-equilibrium steady state and induced currents of a mesoscopically-glassy system: interplay of resistor-network theory and Sinai physics

Daniel Hurowitz[1], Saar Rahav[2], Doron Cohen[1]

[1]*Department of Physics, Ben-Gurion University of the Negev, Beer-Sheva, Israel*
[1]*Schulich Faculty of Chemistry, Technion - Israel Institute of Technology, Haifa 32000, Israel*

We introduce an explicit solution for the non-equilibrium steady state (NESS) of a ring that is coupled to a thermal bath, and is driven by an external hot source with log-wide distribution of couplings. Having time scales that stretch over several decades is similar to glassy systems. Consequently there is a wide range of driving intensities where the NESS is like that of a random walker in a biased Brownian landscape. We investigate the resulting statistics of the induced current I. For a single ring we discuss how the sign of I fluctuates as the intensity of the driving is increased, while for an ensemble of rings we highlight the fingerprints of Sinai physics on the distribution of the absolute value of I.

I. INTRODUCTION

The transport in a chain due to random non-symmetric transition probabilities is a fundamental problem in statistical mechanics [1–7]. This type of dynamics is of great relevance for surface diffusion [8], thermal ratchets [9–12] and was used to model diverse biological systems, such as molecular motors, enzymes, and unidirectional motion of proteins along filaments [13–16]. Of particular interest are applications that concern the conduction of DNA segments [17, 18], and thin glassy electrolytes under high voltages [19–23].

Mathematically one can visualize the dynamics as a *a random-walk in a random environment*: a particle that makes incoherent jumps between "sites" of a network. In an unbounded quasi-one-dimensional network we might have either diffusion or sub-diffusive Sinai spreading [6], depending on whether the transitions rates form a symmetric matrix or not. In contrast, when the system is bounded (and without disjoint components) it eventually reaches a well-defined steady state. This would be an equilibrium *canonical* (Boltzmann) state if the transition rates were detailed-balanced, else it is termed non-equilibrium steady state (NESS).

Considering the NESS of a mesoscopically glassy system, *our working hypothesis is that glassiness might lead to a novel NESS with fingerprints of Sinai physics.* By "glassiness" we mean that the rates that are induced by a bath, or by an external source, have a log-wide distribution, hence many time scales are involved [24] as in spin-glass models [25]. Having a log-wide distribution of time scales is typical for hopping in a random energy landscape, where the rates depend exponentially on the barrier heights. It also arises in driven quasi-integrable systems, where due to approximate selection-rules there is a "sparse" fraction of large coupling-elements, while the majority become very small [26].

The emergence of Sinai physics in a system that is described by a rate equation with asymmetric transition probabilities is not self-evident [27]. An experimental observation of Sinai diffusion regarding the unzipping transition of DNA molecules has been reported [28], and

other applications have been considered [29, 30]. The non-linear current dependence of a mesoscopic rings has been theoretically studied in the past [19, 23], with references to experiments [20–22], *but the statistical aspects, and the possible relevance of Sinai physics, have not been considered.* In previous publications, we have pointed out that due to "glassiness" Sinai physics becomes a relevant ingredient in the analysis of energy absorption [31] and transport [32] in such a ring system.

In this work we consider a geometrically closed mesoscopic system that has a non-trivial topology. The system is immersed in a finite temperature "cold" bath. Additionally it is coupled to a driving-source, with couplings that are log-wide distributed. The driving-source can be regarded as a "hot bath" of infinite temperature. Consequently detailed-balance is spoiled, and after a transient a NESS is reached. Specifically we consider the simplest possible model: a mesoscopic ring that is made up of N sites. See Fig.1 for a graphical illustration. Due to the lack of detailed-balance a circulating current is induced. We shall see that the value of the current (I) depends in a non-linear way on the intensity (ν) of the driving source. Our interest is in the statistical aspects of this dependence.

Our model is physically motivated and significantly differs from the standard setup that has been assumed in past literature. Previous study of Sinai-type disordered systems [7], has considered an open geometry with uncorrelated transition rates that have the same coupling everywhere. Consequentially the random-resistor-network aspect (which is related to local variation of the couplings) has not emerged. Furthermore, in the physically motivated setup that we have defined above (ring+bath+driving) Sinai physics would not arise if the couplings to the driving source were merely disorderly random. The log-wide distribution is a crucial ingredient. Finally, in a closed (ring) geometry, unlike an open (two terminal) geometry, the statistics of I is not only affected by the distribution of transition rates, but also by the spatial profile of the NESS. This is like "canonical" as opposed to "grand canonical" setting, leading to remarkably different results.
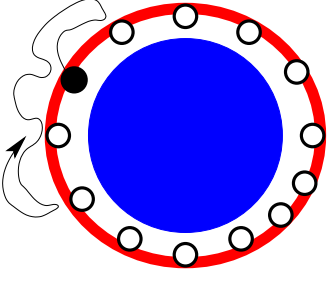
FIG. 1: Schematic illustration of the model system. A ring made up of N sites is immersed in a "cold" bath (represented by inner blue circle) and subjected to a "hot" driving source (represented by an outer red circle). The latter has an intensity ν that can be easily controlled experimentally. The transitions rates between the sites of the ring are given by Eq.(1). The dynamics can be optionally regarded as that of a random walker in a random environment. After a transient a NESS is reached with current $I(\nu)$.

Outline.– In Sec. II we describe our minimal model: a ring coupled to a heat bath and to a driving field, with log-wide distribution of coupling. In Sec. III we estimate the number of sign changes of the steady state current $I(\nu)$ as the intensity of the driving is increased. In Secs. IV and V we present an explicit formula for the NESS. This formula is employed in Sec. VI to study the statistical properties of $I(\nu)$ for an ensemble of rings. Specifically, the statistics outside of the Sinai regime is investigated in Sec.VII, while the statistics in the Sinai regime is studied in Sec.VIII. In the latter case we show how the fingerprints of Sinai physics can be extracted from the analysis of $I(\nu)$ curves. The results are summarized in Sec. IX.

II. THE MODEL

Consider a ring that consists of sites labeled by n with positions $x = n$ that are defined modulo N. The bonds are labeled as $\overrightarrow{n} \equiv (n-1 \rightsquigarrow n)$. The inverse bond is $\overleftarrow{n}$, and if direction does not matter we label both by $\bar{n}$. The position of the nth bond is defined as $x_n \equiv n-(1/2)$. The on-site energies E_n are normally distributed over a range Δ, and the transitions rates are between nearest-neighboring sites:

$$w_{\overrightarrow{n}} = w^{\beta}_{\overrightarrow{n}} + \nu g_{\bar{n}} \tag{1}$$

Here w^{β} are the rates that are induced by a bath that has a finite temperature T_B. The $g_{\bar{n}}$ are couplings to a driving source that has an intensity ν. These couplings are log-box distributed within $[g_{\min}, g_{\max}]$. This means that $\ln(g_{\bar{n}})$ are distributed uniformly over a range $\sigma = \ln(g_{\max}/g_{\min})$. The bath transition rates satisfy detailed-balance, namely

$$\frac{w^{\beta}_{\overrightarrow{n}}}{w^{\beta}_{\overleftarrow{n}}} = \exp\left[-\frac{E_n - E_{n-1}}{T_B}\right] \tag{2}$$

Assuming $\Delta \ll T_B$ one obtains the following approximation:

$$w^{\beta}_{\overrightarrow{n}} \approx \left[1 - \frac{1}{2}\left(\frac{E_n - E_{n-1}}{T_B}\right)\right]\bar{w}^{\beta}_{\bar{n}} \tag{3}$$

$$w^{\beta}_{\overleftarrow{n}} \approx \left[1 + \frac{1}{2}\left(\frac{E_n - E_{n-1}}{T_B}\right)\right]\bar{w}^{\beta}_{\bar{n}} \tag{4}$$

The driving spoils the detailed-balance. We define the resulted stochastic field as follows:

$$\mathcal{E}(x_n) \equiv \ln\left[\frac{w_{\overrightarrow{n}}}{w_{\overleftarrow{n}}}\right] \tag{5}$$

Assuming $\Delta \ll T_B$ we get the following approximation:

$$\frac{w_{\overrightarrow{n}}}{w_{\overleftarrow{n}}} = \frac{w^{\beta}_{\overrightarrow{n}} + \nu g_{\bar{n}}}{w^{\beta}_{\overleftarrow{n}} + \nu g_{\bar{n}}} \approx 1 - \frac{(E_n - E_{n-1})/T_B}{1 + (g_{\bar{n}}/\bar{w}^{\beta}_{\bar{n}})\nu} \tag{6}$$

leading to

$$\mathcal{E}(x_n) \approx -\left[\frac{1}{1 + g_{\bar{n}}\nu}\right]\frac{E_n - E_{n-1}}{T_B} \tag{7}$$

In the last equality, without loss of generality, the $g_{\bar{n}}$ have been re-scaled such that all the bath-induced transitions have the same average value $\bar{w}^{\beta} = 1$.

III. CURRENT SIGN REVERSALS IN THE SINAI REGIME

The direction of the current $\text{sign}(I)$ is determined by the stochastic motive force (SMF), also known as the affinity, or as the entropy production [33–36]:

$$\mathcal{E}_{\circlearrowleft} \equiv \ln\left[\frac{\prod_n w_{\overrightarrow{n}}}{\prod_n w_{\overleftarrow{n}}}\right] = \oint \mathcal{E}(x)\,dx \tag{8}$$

In the second equality we formally regard x as a continuous variable. This will make the later mathematics more transparent. Assuming $\Delta \ll T_B$ we get the following approximation:

$$\mathcal{E}_{\circlearrowleft} \approx -\sum_{n=1}^{N}\left[\frac{1}{1 + g_{\bar{n}}\nu}\right]\frac{\Delta_n}{T_B} \tag{9}$$

One observes that for $\nu \ll g_{\max}^{-1}$ the SMF is linear $\mathcal{E}_{\circlearrowleft} \propto \nu$, while for $\nu \gg g_{\min}^{-1}$ it vanishes $\mathcal{E}_{\circlearrowleft} \propto 1/\nu$. In the intermediate regime, which we call below *the Sinai regime*, the SMF changes sign several times, see Fig. 2. Using the notations

$$\tau \equiv \frac{1}{\sigma}\ln(g_{\max}\nu) \tag{10}$$

and $\tau_n = (1/\sigma)\ln(g_{\max}/g_{\bar{n}})$, the expression for the SMF takes the following form:

$$\mathcal{E}_{\circlearrowleft}(\tau) = -\sum_{n=1}^{N} f_{\sigma}(\tau - \tau_n)\frac{E_n - E_{n-1}}{T_B} \tag{11}$$
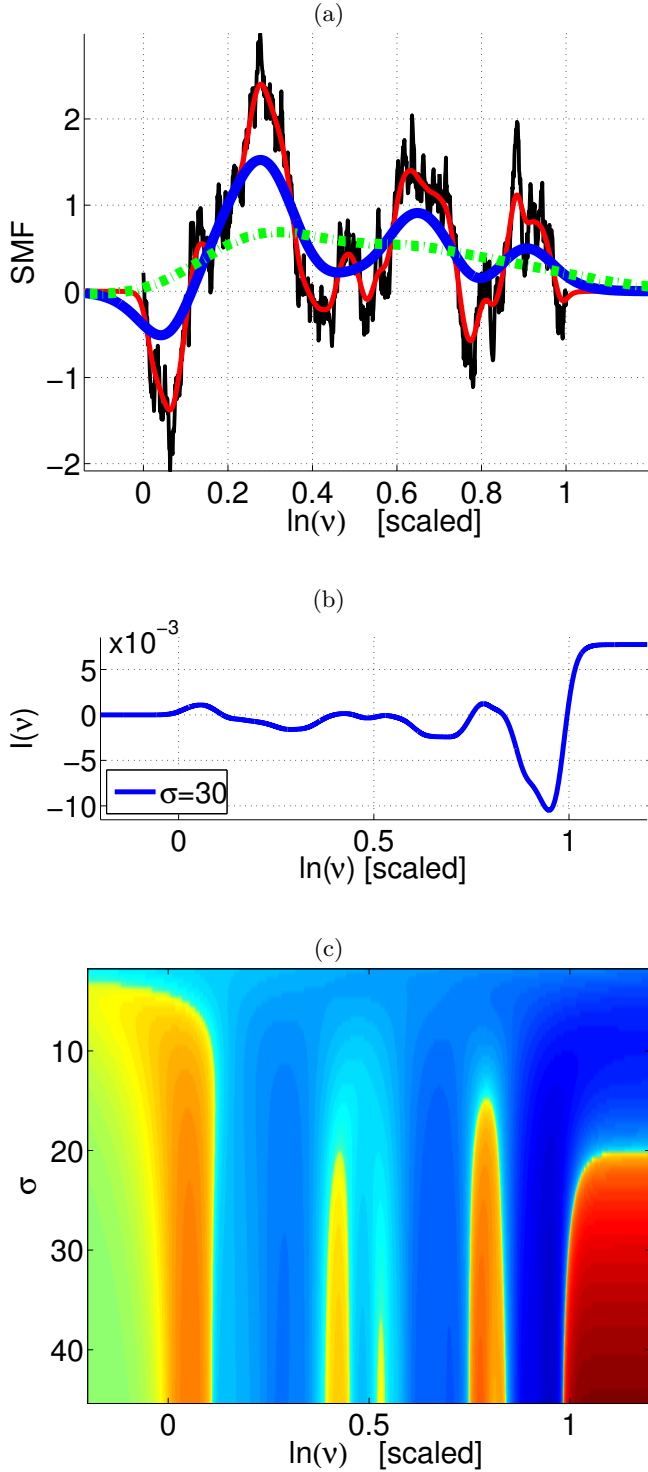
where $f_\sigma(t) \equiv [1+e^{\sigma t}]^{-1}$ drops monotonically from unity to zero like a smoothed step function. If $f(t)$ were a sharp step function it would follow that in the Sinai regime $\mathcal{E}_{\circlearrowright}(\tau)$ is formally like a random walk [37–39]. The number of sign reversals equals the number of times the random walker crosses the origin. We have here a coarse-grained random walk: the τ_n are distributed uniformly over a range $[0,1]$, and each step is smoothed by $f_\sigma(t)$ such that the effective number of coarse-grained steps is σ. Hence we expect the number of sign changes to be not $\sim \sqrt{\pi N}$ but $\sim \sqrt{\pi\sigma}$, reflecting the log-width of the distribution.

IV. ADDING BONDS IN SERIES

The NESS equations are quite simple and can be solved using elementary algebra as in [19, 20, 23, 32], or optionally using the network formalism for stochastic systems [40–42]. Below we propose a generalized resistor-network approach that allows to obtain a more illuminating version for the NESS, that will provide better insight for the statistical analysis. Let us assume that we have a NESS with a current I. The steady state equations for two adjacent bonds are

$$I = w_{\overrightarrow{1}}p_0 - w_{\overleftarrow{1}}p_1 \tag{12}$$

$$I = w_{\overrightarrow{2}}p_1 - w_{\overleftarrow{2}}p_2 \tag{13}$$

We can combine them into one equation:

$$I = \overrightarrow{G}p_0 - \overleftarrow{G}p_2, \tag{14}$$

with

$$\overrightarrow{G} \equiv \left[\frac{1}{w_{\overrightarrow{1}}} + \frac{1}{w_{\overrightarrow{2}}}\left(\frac{w_{\overleftarrow{1}}}{w_{\overrightarrow{1}}}\right)\right]^{-1} \tag{15}$$

$$\overleftarrow{G} \equiv \left[\frac{1}{w_{\overleftarrow{2}}} + \frac{1}{w_{\overleftarrow{1}}}\left(\frac{w_{\overrightarrow{2}}}{w_{\overleftarrow{2}}}\right)\right]^{-1} \tag{16}$$

We can repeat this procedure iteratively. If we have N bonds in series we get

$$\overrightarrow{G} = \left[\sum_{m=1}^{N} \frac{1}{w_{\overrightarrow{m}}} \exp\left(-\int_0^{m-1}\mathcal{E}(x)dx\right)\right]^{-1} \tag{17}$$

$$\overleftarrow{G} = \left[\sum_{m=1}^{N} \frac{1}{w_{\overleftarrow{m}}} \exp\left(\int_m^{N}\mathcal{E}(x)dx\right)\right]^{-1} \tag{18}$$

Coming back to the ring, we can cut it at an arbitrary site n, and calculate the associated Gs. It follows that $I = (\overrightarrow{G}_n - \overleftarrow{G}_n)\,p_n$. Consequently the NESS is

$$p_n = \frac{I}{\overrightarrow{G}_n - \overleftarrow{G}_n} \tag{19}$$

and I can be regarded as the normalization factor:

$$I = \left[\sum_{n=1}^{N} \frac{1}{\overrightarrow{G}_n - \overleftarrow{G}_n}\right]^{-1} \tag{20}$$

FIG. 2: We consider a ring with $N = 1000$ sites whose energies are normally distributed with dispersion $\Delta = 1$. The bath temperature is $T_B = 10$. In (a) the SMF of Eq.(11) is plotted for $\sigma = \infty$, and for $\sigma = 50, 10, 4$. The smaller σ, the smoother ν dependence. In (b) a representative $I(\nu)$ curve is plotted. In (c) a set of $I(\nu)$ curves is color-imaged: each row is $I(\nu)$ for a different σ, blue and red are for positive and negative (clockwise) circulating current respectively. In all panels the horizontal axis is the scaled driving intensity as defined in Eq.(10).
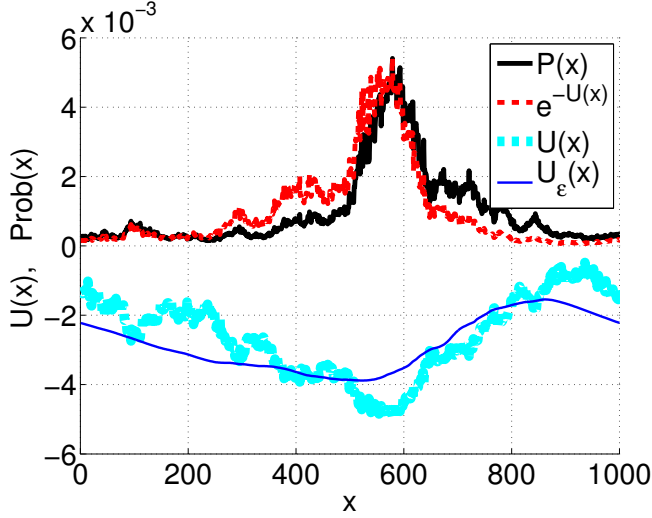
FIG. 3: The NESS profile of Eq.(26) (solid black) is similar but not identical to the quasi-equilibrium distribution (dashed red line). Also shown (lower curves) is the potential landscape $U(x)$ and its smoothed version $U_\varepsilon(x)$. The parameters are the same as in Fig.2, with $\sigma = 10$, and driving intensity that corresponds to $\tau = 0.3$. The bonds were re-arranged to have a larger SMF, namely $\mathcal{E}_{\circlearrowleft} = 7.4$.

In the next paragraph we show how to write these results in an explicit way that illuminates the relevant physics.

V. THE NESS FORMULA

One should notice that Eq.(17) and Eq.(18) cannot be treated on equal footing due to a miss-match between m and $m-1$. For this reason we introduced an improved convention for the description of the bonds. We define the conductance of a bond as the geometric mean of the clockwise and anticlockwise transition rates:

$$w(x_n) = \sqrt{w_{\overrightarrow{n}} w_{\overleftarrow{n}}} \qquad (21)$$

Hence $w_{\overrightarrow{n}} = w(x_n) \exp[(1/2)\mathcal{E}(x_n)]$. Accordingly Eq.(17) and Eq.(18) can be unified and written as

$$\overrightarrow{G}_n = \left[\sum_{m=n+1}^{N+n} \frac{1}{w(x_m)} \exp\left(-\int_n^{x_m} \mathcal{E}(x) dx \right) \right]^{-1} \qquad (22)$$

Where the implicit understanding is that the summation and the integration are anticlockwise modulo N. With the new notations it is easy to see that $\overleftarrow{G}_n = \exp(-\mathcal{E}_{\circlearrowleft}) \overrightarrow{G}_n$. We use the notation G_n for the geometric mean. Consequently the formula for the current takes the form

$$I = \left[\sum_{n=1}^{N} \frac{1}{G_n} \right]^{-1} 2\sinh\left(\frac{\mathcal{E}_{\circlearrowleft}}{2} \right) \qquad (23)$$

while $p_n \propto 1/G_n$. Our next task is to find a tractable expression for the latter. Regarding x as an extended coordinate, the potential $V(x)$ that is associated with the field $\mathcal{E}(x)$ is a tilted periodic potential. Adding $[\mathcal{E}_{\circlearrowleft}/N]x$ we get a periodic potential $U(x)$, see Fig.3. Accordingly

$$\int_{x'}^{x''} \mathcal{E}(x) dx = U(x') - U(x'') + \frac{\mathcal{E}_{\circlearrowleft}}{N}(x'' - x') \qquad (24)$$

With any function $A(x)$ we can associate a smoothed version using the following definition

$$\sum_{r=1}^{N} A(x+r) e^{U(x+r) - (1/N)\mathcal{E}_{\circlearrowleft} r} \equiv A_\varepsilon(x) e^{U_\varepsilon(x)} \qquad (25)$$

In particular the smoothed potential $U_\varepsilon(x)$ is defined by this expression with $A = 1$. Note that without loss of generality it is convenient to have in mind $\mathcal{E}_{\circlearrowleft} > 0$. (One can always flip the x direction). Note also that the smoothing scale $N/\mathcal{E}_{\circlearrowleft}$ becomes larger for smaller SMF. With the above definitions we can write the NESS expression as follows:

$$p_n \propto \left(\frac{1}{w(x_n)} \right)_\varepsilon e^{-(U(n) - U_\varepsilon(n))} \qquad (26)$$

This expression is physically illuminating, see Fig.3. In the limit of zero SMF it coincides, as expected, with the canonical (Boltzmann) result. For finite SMF the smoothed pre-factor and the smoothed potential are not merely constants. Accordingly the pre-exponential factor becomes important and the "slow" modulation by the Boltzmann factor is flattened. If we take the formal limit of infinite SMF the Boltzmann factor disappears and we are left with $p_n \propto 1/w_n$ as expected from the continuity equation for a resistor-network.

VI. STATISTICS OF THE CURRENT

From the preceding analysis it should become clear that the formula for the current can be written schematically as

$$I(\nu) \sim \frac{1}{N} w_\varepsilon e^{-B} 2\sinh\left(\frac{\mathcal{E}_{\circlearrowleft}}{2} \right) \qquad (27)$$

In the absence of a potential landscape ($U(x) = 0$) the formula becomes equivalent to Ohm law: it is a trivial exercise to derive it if all anticlockwise and clockwise rates are equal to the same values $\overrightarrow{w}$ and $\overleftarrow{w}$ respectively, hence $w_\varepsilon = (\overrightarrow{w} \overleftarrow{w})^{1/2}$, and $\mathcal{E}_{\circlearrowleft} = N \ln(\overrightarrow{w}/\overleftarrow{w})$. In the presence of a potential landscape we have an activation barrier. Assuming that the current is dominated by the highest peak a reasonable estimate would be

$$B = \max\{U(x) - U_\varepsilon(x)\} \qquad (28)$$

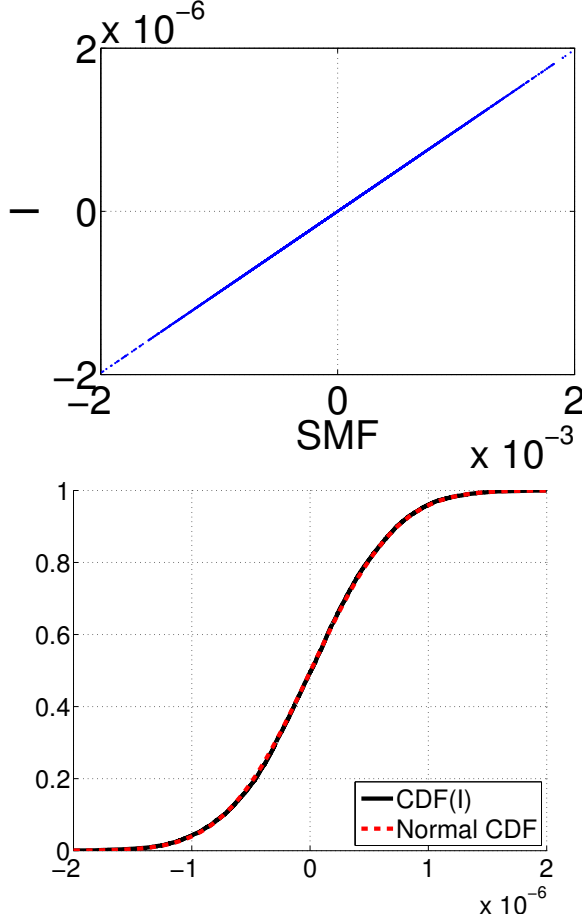$$\approx \frac{1}{2}\Big[\max\{U\} - \min\{U\}\Big] \qquad (29)$$

FIG. 4: In the linear regime, the current is strongly correlated with the SMF (uppper panel), and consequently it has *normal* statistics (lower panel). For the statistical analysis we have generated 10^5 realizations of the ring with $\sigma = 6$.

VII. STATISTICS OF CURRENT OUTSIDE OF THE SINAI REGIME

As the driving intensity is increased one observes a crossover from a linear regime, to a Sinai regime, and finally a saturation regime:

$$
\begin{array}{lll}
\text{Linear regime:} & \nu < g_{max}^{-1} & (30) \\
\text{Sinai regime:} & g_{max}^{-1} < \nu < g_{min}^{-1} & (31) \\
\text{Saturation regime:} & \nu > g_{min}^{-1} & (32)
\end{array}
$$

Consequently we get for the SMF the following approximations:

$$
\mathcal{E}_{\circlearrowleft} \approx \frac{1}{T_B}
\begin{cases}
\Delta^{(0)} \nu, & \text{Linear regime} \\
-\Delta^{(\infty)}/\nu, & \text{Saturation regime}
\end{cases}
\quad (33)
$$

where

$$
\Delta^{(0)} \equiv \sum_n g_{\bar{n}} \Delta_n \sim \pm \left[2N \operatorname{Var}(g) \right]^{1/2} \Delta \quad (34)
$$

$$
\Delta^{(\infty)} \equiv \sum_n \frac{1}{g_{\bar{n}}} \Delta_n \sim \pm \left[2N \operatorname{Var}(g^{-1}) \right]^{1/2} \Delta \quad (35)
$$

The estimates for $\Delta^{(0)}$ and for $\Delta^{(\infty)}$ follow from the observation that we have sums of independent random variables. For example $\Delta^{(0)}$ can be re-arranged as $\sum_{n=1}^{N} (g_{\bar{n}+1} - g_{\bar{n}}) E_n$. Furthermore, we conclude that both $\Delta^{(0)}$ and $\Delta^{(\infty)}$ have *normal* statistics as implied by the central limit theorem. Consequently we expect *normal* statistics for the SMF, and hence for the current, as verified in Fig. 4.

VIII. STATISTICS IN THE SINAI REGIME

We now focus on the statistics in the Sinai regime. In order to unfold the log-wide statistics it is not a correct procedure to plot blindly the distribution of $\ln(|I|)$. Rather one should look on the joint distribution $(\mathcal{E}_{\circlearrowleft}, I)$. See Fig. 5a. The non-trivial statistics is clearly apparent. In order to describe it analytically we use the single-barrier estimate of Eq. (28), which is tested in Fig. 5b. We see that it over-estimates the current for small B values (flat landscape) as expected, but it can be trusted for large B where the Sinai physics becomes relevant.

In Fig. 6 we confirm that the probability distribution of the current $P(I; \text{SMF})$, for a given SMF, is the same as the barrier $\exp(-B)$ statistics. We therefore turn to find an explicit expression for the latter.

The probability to have a random walk trajectory $X_n = U(x_n)$ within $[X_a, X_b]$ equals the survival probability in a diffusion process that starts as a delta function at $X = 0$ with absorbing boundary conditions at X_a and X_b. Integrating over all possible positions of the walls such that $X_b - X_a = R$ is like starting with a uniform distribution between the walls. From here it is straightforward to deduce what is the probability distribution function $f(R)$. The result is displayed in Fig. 7. For the derivation of the exact expression see Appendix A. We note that the occupation-range statistics $f(R)$ is very different from that of maximal-distance statistics $f(K)$, see Appendix B.
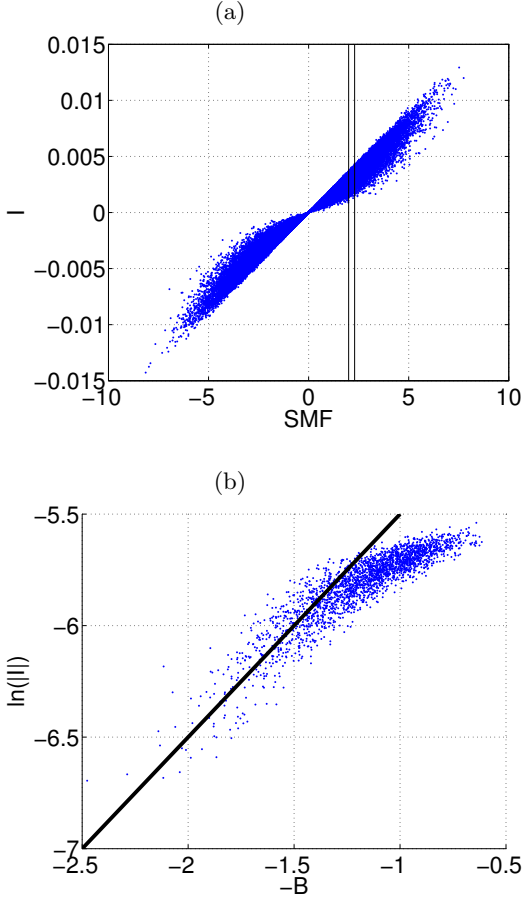
The implication of Eq. (27) with Eq. (28) for the *statistics* of the current is as follows: in the Sinai regime we expect that it will reflect the *log-wide* distribution of the activation factor, while outside of the Sinai regime we expect it to reflect the *normal* distributions of the total resistance w_ε^{-1}, and of the SMF.

In the following sections we provide a detailed analysis for the statistics of $I(\nu)$. We shall see that contrary to first impression the extraction of the fingerprints of the log-normal statistics in the Sinai regime requires extra treatment. The bare statistics is in fact normal in all regimes.
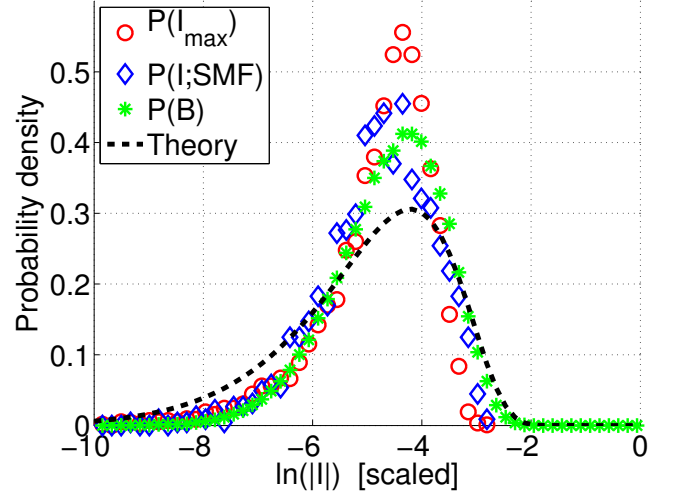
FIG. 6: The log-wide distribution $P(I)$ of the current in the Sinai regime is revealed provided a proper procedure is adopted. For theoretical analysis it is convenient to plot an histogram of the I values for a given SMF: the blue diamonds refer to the data of Fig. 5b. In an actual experiment it is desired to extract statistics from $I(\nu)$ measurements without referring to the SMF: the red empty circles show the statistics of the first maximum of $I(\nu)$. Both distributions look the same, and reflect the barrier statistics (full green circles). The line is the exact version of Eq.(37).

FIG. 5: (a) Scatter diagram of the current versus the SMF in the Sinai regime. Note that in the linear regime, see Fig.4, it looks like a perfect linear correlation with *negligible* transverse dispersion. (b) The correlation between the current I and the barrier B, within the slice $\mathcal{E}_{\circlearrowleft} \in [2.0, 2.1]$. One deduces that the single-barrier approximation is valid for small currents.

Turning back to the problem under consideration, Eq.(29) implies that the probability to have a barrier B is the same as the probability that $U(x)$ occupies a range $R = 2B$. Hence it is described by the probability distribution function $f(R)$ of Fig. 7. The derivation in Appendix A leads to the following practical expression,

$$\text{Prob}\{\text{barrier} < B\} \ \sim \ \exp\left[-\frac{1}{2}\left(\frac{\pi\sigma_U}{2B}\right)^2\right] \quad (36)$$

where the variance $\sigma_U^2 = 2DN$ is determined by the diffusion coefficient $D \propto \Delta^2$ that characterizes the potential landscape, see for example the illustration in Fig.3. Taking into account that for a given ν a fraction of the elements in Eq.(11) are effectively zero we get

$$\sigma_U^2 \ = \ 2\Delta^2 N \frac{\ln(g_{max}\nu)}{\sigma} \quad (37)$$

The validity of the exact version of Eq. (36), which is based Eq.(A11) of Appendix A, has been verified in Fig.5. No fitting parameters are required.
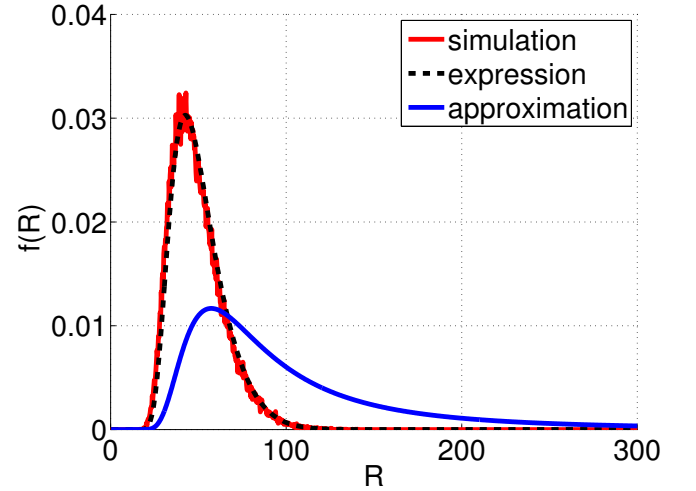

FIG. 7: Plot of $f(R)$. Red line is the outcome of a random walk simulation with $t = 1000$ steps that are Gaussian distributed with unit dispersion. The black dashed line is the exact result Eq.(A11), while the lower (blue) solid line is from the simple asymptotic approximation Eq.(A13).

In an actual experiment it would be desired to extract the statistics from the $I(\nu)$ measurements without referring to the SMF. In Fig. 6 we show that the statistics of the first maximum of $I(\nu)$ is practically the same as $P(I; \text{SMF})$. This means that a simple statistical analysis of "current versus irradiation" curves is enough in order

to reveal the fingerprints of Sinai-type physics.

IX. SUMMARY

We have introduced a generalized "random-resistor-network" approach for the purpose of obtaining the NESS current due to nonsymmetric transition rates. Specifically our interest was focused on the NESS of a "glassy" mesoscopic system. The NESS expression clearly interpolates the canonical (Boltzmann) result that applies in equilibrium, with the resistor-network result, that applies at infinite temperature. Due to the "glassiness" the current has novel dependence on the driving intensity, and it posseses unique statistical properties that reflect the Brownian landscape of the stochastic potential. This statistics is related to Sinai's random walk problem, and would not arise if the couplings to the driving source were merely disordered.

From the point of view of a practical experiment, we have assumed that the most accessible measurements would be "current vs irradiation" curves ($I(\nu)$). Namely, experiments in which one changes the external driving intensity and observe changes in the resulting NESS. The Sinai regime manifests in sign reversals of the current, whose number is estimated in Sec. III.

By repeating such experiments with an ensemble of macroscopically equivalent rings one may find imprints of the Sinai regime in the statistics of the NESS current. Our results, depicted in Fig. 6, suggest that from $I(\nu)$ measurements alone one can extract valuable information regarding the Brownian landscape of the stochastic potential; The functional shape of the distribution provides an indication for having Sinai-type physics; while from its width one can extract the characteristic parameters of the disorder.

[1] B. Derrida, Y. Pomeau, Phys. Rev. Lett. 48, 627 (1982).

[2] S. H. Noskowicz, I. Goldhirsch, Phys. Rev. Lett. 61, 500 (1988); Phys. Rev. A 42, 2047 (1990).

[3] J. P. Bouchaud, A. Comtet, A. Georges, P. Le Doussal, Ann. Phys. (N.Y.) 201, 285 (1990).

[4] H. E. Roman, M. Schwartz, A. Bunde, S. Havlin, Europhys. Lett. 7, 389 (1988).

[5] D. Fisher, P. Le Doussal, and C. Monthus, Phys. Rev. Lett. 80, 3539 (1998).

[6] Ya. G. Sinai, Theory Probab. Its Appl. 27, 247 (1982)

[7] S.F. Burlatsky, G.S. Oshanin, A.V. Mogutov, M. Moreau, Phys. Rev. A 45, R6955 (1992).

[8] R. L. Schwoebel and E. J. Shipsey, J. Appl. Phys. 37, 3682 (1966)

[9] M. O. Magnasco, Phys. Rev. Lett. 71, 1477 (1993)

[10] R. D. Astumian and M. Bier, Phys. Rev. Lett. 72, 1766 (1994)

[11] M. O. Magnasco, Phys. Rev. Lett. 72, 2656 (1994)

[12] P. Reimann, Phys. Rep. 361, 57 (2002)

[13] C.T. MacDonald, J.H. Gibbs and A.C. Pipkin, Biopolymers, 6, 1 (1968)

[14] H. X. Zhou and Y. D. Chen, Phys. Rev. Lett. 77, 194 (1996)

[15] E. Frey and K. Kroy, Ann. Phys. 14, 20 (2005)

[16] A.B. Kolomeisky and M.E. Fisher, Annu. Rev. Phys. Chem. 58, 675 (2007)

[17] B. Xu, P. Zhang, X. Li and N. Tao, Nano Lett. 4, 1105 (2004)

[18] H. W. Fink and C. Schönenberger, Nature 398, 407 (1999)

[19] K. W. Kehr, K. Mussawisade, and T. Wichmann, Phys. Rev. E 56, R2351 (1997).

[20] A. Heuer, S. Murugavel, and B. Roling, Phys. Rev. B 72, 174304 (2005).

[21] S. Murugavel and B. Roling, J. Non-Cryst. Solids 351, 2819 (2005).

[22] B. Roling, S. Murugavel, A. Heuer, L. Luhning, R. Friedrich and S. Rothel, Phys. Chem. Chem. Phys. 10, 4211 (2008).

[23] M. Einax, M. Korner, P. Maass, A. Nitzan, Phys. Chem. Chem. Phys. 12, 645 (2010).

[24] F. Ritort, P. Sollich, Adv. Phys. 52, 219 (2003)

[25] A. Crisanti, F. Ritort, J. Phys. A 36, R181 (2003)

[26] D. Cohen, Physica Scripta T151, 014035 (2012), and further references therein.

[27] M. Sales, J.-P. Bouchaud, F. Ritort, J. Phys. A 36, 665 (2003)

[28] D. Lubensky, D. Nelson, Phys. Rev. E 65, 031917 (2002)

[29] F. Corberi, A. De Candia, E. Lippiello, M. Zannetti, Phys. Rev. E 65, 046114 (2002)

[30] S. Luding, M. Nicolas, O. Pouliquen, p.241 in: Compaction of Soils, Granulates and Powders, edited by D. Kolymbas and W. Fellin (Balkema Rotterdam 2000).

[31] D. Hurowitz, D. Cohen, Europhysics Letters 93, 60002 (2011)

[32] D. Hurowitz, S. Rahav, D. Cohen, Europhysics Letters 98, 20002 (2012)

[33] J. L. Lebowitz and H. Spohn, J. Stat. Phys. 95, 333 (1999).

[34] P. Gaspard, J. Chem. Phys., 120, 8898 (2004).

[35] Udo Seifert, Phys. Rev. Lett. 95, 040602 (2005)

[36] D. Andrieux and P. Gaspard, J. Stat. Phys., 127, 107 (2007).

[37] Adrienne W. Kemp, Adv. Appl. Probab. 19, 505 (1987).

[38] W. Feller, An Introduction to Probability Theory and its Applications (Wiley, New York, 1950)

[39] M. Dwass, Ann. Math. Stat. 38, 1042 (1967)

[40] J. Schnakenberg, Rev. Mod. Phys. 48, 571 (1976).

[41] T.L. Hill, J. Theor. Biol. v10, 442 (1966)

[42] R. K. P. Zia and B. Schmittmann, J. Stat. Mech. (2007), P07012.

Appendix A: Random-walk occupation-range statistics

In this section we derived the probability density function $f(R)$ to have a random walk process $x(\cdot)$ of t steps that occupies a range R. This is determined by the probability

$$P_t(x_a, x_b) \equiv \text{Prob}\Big(x_a < x(t') < x_b \ \text{ for any } t' \in [0,t]\Big) \tag{A1}$$

Accordingly the joint probability density that a random walker would occupy an interval $[x_a, x_b]$ is

$$f(x_a, x_b) = -\frac{d}{dx_a}\frac{d}{dx_b} P_t(x_a, x_b) \tag{A2}$$

It is convenient to use the coordinates

$$X = \frac{x_a + x_b}{2} \tag{A3}$$

$$R = x_b - x_a \tag{A4}$$

Consequently the expression for $f(R)$ is

$$f(R) = \int_{-\infty}^{0}\int_{0}^{\infty} dx_a dx_b \ f(x_a, x_b) \ \delta\left(R - (x_b - x_a)\right) \tag{A5}$$

$$f(R) = -\int_{-R/2}^{R/2} \left(\frac{1}{4}\partial_X^2 - \partial_R^2\right) P_t(R, X) \ dX \tag{A6}$$

Taking into account that $P_t(R, X)$ and its derivatives vanish at the endpoints $X = \pm(R/2)$ we get

$$f(R) = \int_{-R/2}^{R/2} \partial_R^2 \ P_t(R, X) \ dX = \partial_R^2 \Big[R \ P_t(R)\Big] \tag{A7}$$

where $P_t(R)$ is the survival probability of a diffusion process that starts with an initial *uniform* distribution, instead of a random walk that starts as a delta distribution. Optionally we can write

$$\text{Prob(range} < R) = \partial_R \Big[R \ P_t(R)\Big] \tag{A8}$$

We now turn to find an explicit expression for $P_t(R)$. This is done by solving the diffusion equation. Using Fourier expansion the solution is

$$\rho_t(x) = \sum_{n=1,3,5,\dots}^{\infty} \exp\left[-D\left(\frac{\pi n}{R}\right)^2 t\right] \frac{4}{\pi n R} \sin\left(\frac{\pi n}{R}x\right) \tag{A9}$$

For simplicity we have shifted above the domain to $x \in [0, R]$. For the survival probability we get

$$P_t(R) = \int_0^R \rho_t(x) \ dx = \sum_{n=1,3,5,\dots}^{\infty} \frac{8}{\pi^2 n^2} \exp\left[-D\left(\frac{\pi n}{R}\right)^2 t\right] \tag{A10}$$

Using Eq.(A10) in Eq.(A7) we get

$$f(R) = \frac{8\sigma^2}{R^3} \sum_{n=1,3,5,\dots}^{\infty} \left[\left(\frac{\pi\sigma n}{R}\right)^2 - 1\right] \exp\left[-\frac{1}{2}\left(\frac{\pi\sigma n}{R}\right)^2\right] \tag{A11}$$

This result is in perfect agreement with the numerical simulation of Fig.7. Still we would like to have a more compact expression. One possibility is to keep only the first term. The other possibility is to approximate the summation by an integral:

$$\text{Prob(range} < R) \approx \frac{2}{\pi^2}\frac{\partial}{\partial R}\left[R\int_1^{\infty} \frac{dx}{x^2} \exp\left(-\frac{\pi^2 Dt}{R^2}x^2\right)\right] = \exp\left(-\frac{\pi^2 Dt}{R^2}\right) \tag{A12}$$

Either way we get

$$\text{Prob(range} < R) \sim \exp\left(-\frac{1}{2}\left(\frac{\pi\sigma}{R}\right)^2\right) \tag{A13}$$

where $\sigma^2 = 2Dt$. This asymptotic expression is illustrated in Fig.7. Though it does not work very well, it has the obvious advantage of simplicity.
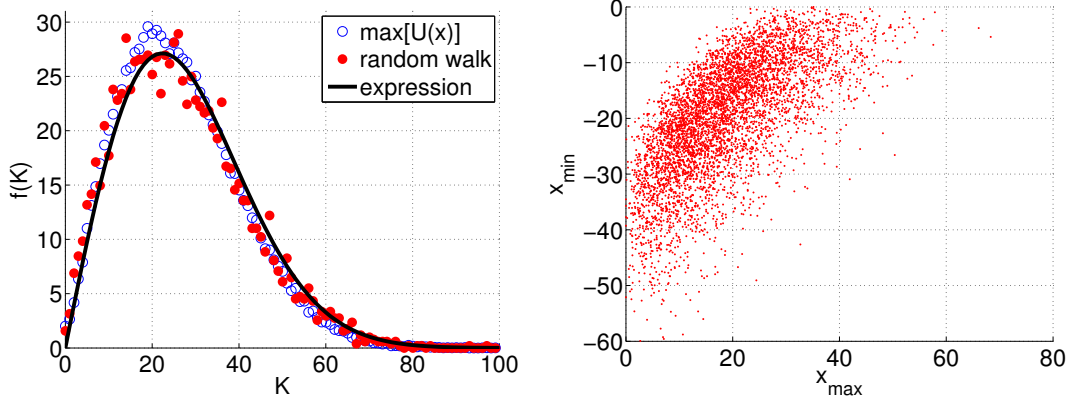
FIG. 8: [Left panel] Plot of $f(K)$. The histogram of $\max[U(x)]$ values over many ring realizations (blue circles) is compared with the K statistics in a constrained random walk process (red points). The analytical result Eq. (B4) is represented by a black line. [Right panel] Scatter plot of $(x_{\min}, x_{\max})$ for the same random walk simulation illustrating the strong correlation.

Appendix B: Random-walk maximal-distance statistics

The occupation-range statistics of the previous section should not be confused with the maximal-distance statistics. The maximal distance from the initial point is defined as follows:

$$K = \max[x(t)], \qquad \text{where } 0 < t < N \tag{B1}$$

Naively, one might think that the probability distribution of K is similar to the probability distribution of R that has been discussed in the previous section. But this is not true. Furthermore, it is also very sensitive to whether the random walk is constrained to end up at the origin, $x(N) = x(0) = 0$. Without the latter constraint $f(K)$ is finite for small K, but if the constraint is taken into account, it vanishes linearly in this limit.

It is the constrained random walk process that describes the potential $U(x)$. The exact result for the the K statistics in this case is known [39]:

$$\text{Prob}(K \geq k; N) = \frac{\binom{2N}{N-k}}{\binom{2N}{N}}, \qquad k = 0, 1, 2 \cdots N \tag{B2}$$

Switching variables to $\kappa = k/N$ and taking the large N limit, one obtains the probability density function

$$f(\kappa) = N \left[\frac{(1-\kappa)^{\kappa-1}}{(1+\kappa)^{\kappa+1}} \right]^N \ln \left[\frac{1+\kappa}{1-\kappa} \right] \tag{B3}$$

which has a peak at $\kappa \sim 1/\sqrt{2N}$. For $\kappa \ll 1$ this expression can be approximated by the simple function. Switching back to K it takes the form

$$f(K) \approx \frac{2K}{N} \exp \left[-\frac{K^2}{N} \right] \tag{B4}$$

In Fig.8a we illustrate this distribution and demonstrate its applicability to the $U(x)$ of the ring model. In Fig.8b we illustrate the joint distribution of the extreme values $x_{\min} = \min[x(\cdot)]$ and $x_{\max} = \max[x(\cdot)]$. The $f(R)$ distribution of the previous section corresponds to its projection along the diagonal direction, while the $f(K)$ distribution of the present section is its projection along the horizontal or vertical directions.